Key residues affecting transglycosylation activity in family 18 chitinases – Insights into donor and acceptor subsites

Jogi Madhuprakash,[1,2] Bjørn Dalhus,[3,4] T. Swaroopa Rani,[2] Appa Rao Podile,[2] Vincent G.H. Eijsink,[1] Morten Sørlie[1].*

[1]Department of Chemistry, Biotechnology and Food Science, Norwegian University of Life Sciences (NMBU), P.O. Box 5003, 1432 Ås, Norway.
[2]Department of Plant Sciences, School of Life Sciences, University of Hyderabad, Gachibowli, Hyderabad, India.
[3]Department of Medical Biochemistry, Institute for Clinical Medicine, University of Oslo, PO Box 4950, Nydalen, N-0424, Oslo, Norway
[4]Department of Microbiology, Clinic for Laboratory Medicine, Oslo University Hospital, Rikshospitalet, PO Box 4950, Nydalen, N-0424, Oslo, Norway

Correspondence address:
Prof. Morten Sørlie,
Faculty of Chemistry, Biotechnology and Food Science,
Norwegian University of Life Sciences (NMBU),
P.O. Box 5003, 1432 Ås,
E-mail: morten.sorlie@nmbu.no

Article type: Original Article

Keywords:
Chitinase, Transglycosylation, Hydrolysis, Chitooligosaccharides, Degree of polymerization.

Abstract

The understanding of features that determine transglycosylation (TG) activity in glycoside hydrolases is important because it would allow the construction of enzymes that can catalyze controlled synthesis of oligosaccharides. To increase TG activity in two family 18 chitinases, chitinase D from *Serratia proteamaculans* (*Sp*ChiD) and chitinase A from *Serratia marcescens* (*Sm*ChiA), we have mutated residues important for stabilizing the reaction intermediate and substrate binding in both donor and acceptor sites. To help mutant design, the crystal structure of the inactive *Sp*ChiD-E153Q mutant in complex with chitobiose was determined. We identified three mutations with a beneficial effect on TG activity: Y28A (affecting the -1 subsite and the intermediate), Y222A (affecting the intermediate) and Y226W (affecting the +2 subsite). Furthermore, exchange of D151, the middle residue in the catalytically important DXDXE motif, to asparagine, reduced hydrolytic activity up to 99 % with a concomitant increase of apparent TG activity. The combination of mutations yielded even higher degrees of TG activity. Reactions with the best mutant, *Sp*ChiD-D151N/Y226W/Y222A, led to rapid accumulation of high levels of TG products that remained stable over time. Importantly, the introduction of analogous mutations at same positions in *Sm*ChiA (Y163A equal to Y28A and Y390F similar to Y22A) had similar effects on TG efficiency. Thus, the combination of reducing hydrolytic power, subsite affinity and the stability of intermediate states provides a powerful, general strategy for creating hypertransglycosylating mutants of retaining glycoside hydrolases.

Introduction

Chitinases catalyze hydrolysis of β-1, 4 glycosidic bonds in chitin, a linear homopolymer of *N*-acetylglucosamine (GlcNAc). Controlled degradation of chitin, and of its partially deacetylated derivative chitosan, yields chitooligosaccharides (CHOS), which are gaining interest due to a wide range of potential biological applications, especially in the food, medical, and agriculture fields[1, 2]. The biological activities of CHOS include antimicrobial activities[3], antitumor properties[4], antifungal activities[5-7], and immuno-enhancing effects[8]. The activity of CHOS depends of their length, degree of acetylation and pattern of acetylation[2]. Despite their interesting properties and potential applications, CHOS with well-defined structures are of limited commercial availability. Most biological activities require CHOS with a degree of polymerization ≥4 and the synthesis of such compounds is a daunting task[9]. Among several methods available for generating CHOS, enzymatic approaches are most promising.

Retaining chitinases belonging to glycoside hydrolase family 18 (GH18) show transglycosylation (TG) activity along with hydrolytic activity, and are thus capable of forming new glycosidic bonds between donor and acceptor saccharides[10-14]. This property may be exploited for the production of longer chain CHOS and may also allow generation of well-defined CHOS by coupling smaller CHOS building blocks[15]. Retaining GHs, catalyze a double displacement reaction[16], which normally involves the formation of a glycosyl-enzyme intermediate. Hydrolysis occurs when a water molecule attacks the glycosyl-enzyme intermediate. Alternatively, a carbohydrate, or another suitable acceptor molecule, outcompetes the water, leading to TG[17]. The GH18 enzymes are special in that catalysis is substrate-assisted; instead of going through a glycosyl-enzyme intermediate, the donor saccharide goes through an oxazolinium ion intermediate that is stabilized by interactions with the enzyme[18-21].

It has been shown that TG activity by chitinases can be improved by mutagenesis. For example, mutation of W167 in the −3 subsite of chitinase A from *Serratia marcescens* (*Sm*ChiA) to alanine enhanced TG activity[22]. Mutations of aspartates in the diagnostic DXDXE sequence motif containing the catalytic glutamic acid in *Sm*ChiA (D311 & D313) and *Sm*ChiB (D140 & D142), which likely affect the stability of the oxazolinium ion intermediate, also improved TG activity[12]. Similar mutations in chitinase-A1 from *Bacillus circulans* WL-12 (*Bc*ChiA1) (D200A

& D202A)[23], chitinase-42 from *Trichoderma harzanium* (D170A & D170N)[23] and chitinase-A from *Vibrio harveyi* (D313A & D313N)[24] also led to improved TG activity. Mutations in the DXDXE motif strongly reduce hydrolytic activity, which, generally, is beneficial for the accumulation of TG products. Furthermore, there is increasing evidence that aromatic side chains in acceptor subsites are important determinants of TG activity in GH18 chitinases[12, 14, 25-27]. In particular, Zakariassen *et al*. (2011)[12] and Umemoto *et al*. (2013, 2015)[26, 27] have shown that TG activity can be enhanced by introducing aromatic side chains in the +2 and +1 subsite of GH18 chitinases, respectively.

Chitinase D, a family 18 chitinase from *Serratia proteamaculans* (*Sp*ChiD) is known for its high TG activity. Although some structural features related to the TG activity of *Sp*ChiD have been identified[13, 14, 28], structural features known to be important for TG from the above-cited studies on other GH18 enzymes have not yet been explored, nor has the potential to generate variants of this promising enzyme that display enhanced TG activity. In the present study, we take advantage of our previous works on *Sm*ChiA and *Sp*ChiD and have carried out an extended mutational study of *Sp*ChiD with the aim of increasing its TG activity. We have assessed the potential of mutations suggested by the above-cited studies on other GH18 chitinases, and we have explored novel mutations that primarily affect the binding of the -1 sugar and the oxazolinium ion intermediate. To help in the mutational design and in the understanding of mutational effects, the X-ray crystal structure of *Sp*ChiD in complex with substrate was determined. Finally, in an attempt to generalize the principles of TG emerging from the work on *Sp*ChiD, analogous mutations were introduced in *Sm*ChiA. This approach yielded variants of both enzymes with strongly enhanced TG activity.

Materials and Methods

Preparation of *Sp*ChiD and *Sm*ChiA mutants −

Wild-type pET-22(b)-*Sp*ChiD was used as template for generating single mutants of *Sp*ChiD, while, pET-22(b)-D151N was used as template for preparing double and triple mutants. *Sm*ChiA-D313N/F396W[12] was used as template for preparing *Sm*ChiA triple mutants. Mutagenesis was performed using the QuikChange II site-directed mutagenesis kit (Agilent Technologies), as described by the manufacturer. The primers and the templates used for mutagenesis are listed in Table 1. The sequences of the mutated genes were confirmed by automated DNA sequencing and

plasmids with desired mutations were transformed into *Escherichia coli* BL21 (DE3) for protein production.

Protein production, isolation and purification −

E. coli BL21 (DE3) cells producing *Sp*ChiD variants were grown as described earlier[29]. Periplasmic fractions were prepared as suggested in the pET expression system manual (Novagen) with minor modifications. In the first step, cells, collected by centrifugation from a 500 mL culture, were resuspended in 15 ml of ice-cold spheroplast buffer and incubated at 4 °C with gentle mixing for 15 min. The spheroplast buffer contained 10 mL of 1 M Tris–HCl, pH 8.0, 20 g sucrose, 200 µL 0.25 M EDTA, pH 8.0, and 200 µL 50 mM phenylmethylsulfonyl fluoride with a final volume adjusted to 100 mL using distilled water. After collection of the cells by centrifugation at 7741 g, for 8 min at 4 °C, the pellet was resuspended in 15 mL of ice-cold filter-sterilized 5 mM $MgSO_4$ solution and incubated at 4 °C for 10 min, followed by centrifugation at 7741 g, for 8 min at 4 °C. The supernatant was sterilized using 0.2 µm filters and used for protein purification. Prior to purification, the protein was transferred to equilibration buffer (50 mM NaH_2PO_4, 300 mM NaCl, 10 mM imidazole), pH 8.0, using Amicon Ultra Centrifugal filters (10 kDa cutoff, Millipore, Billerica, MA). The proteins were purified using standard nickel affinity chromatography, as described previously[29].

*Sm*ChiA variants were isolated by resuspending cells collected by centrifugation in equilibration buffer, followed by sonication at 20 % amplitude with 30 − 5s pulses (with 20s delay between pulses) on ice, using a Vibra cell Ultrasonic Processor, converter model CV33, equipped with a 3 mm probe (Sonics, Newtown, CT, USA). The cell lysate was centrifuged at 15,200 g for 10 min at 4 °C to remove insoluble cell debris and the supernatant was sterilized using 0.2 µm filters before purification as previously described[12]. Fractions with the highest purity were collected and the protein was concentrated using Amicon Ultra Centrifugal filters (10 kDa cutoff, Millipore, Billerica, MA). The protein concentration was measured using the Bradford micro assay supplied by Bio-Rad (CA, USA).

Table 1: Details of primers and templates used for generation of *Sp*ChiD and *Sm*ChiA mutants.

S.No	Name of the mutant	Template used for PCR	Primer combination used	Primer sequence (5'−3')
		***Sp*ChiD Mutants**		
1	Y28A	*Sp*ChiD-WT	Y28A-Fp	CTTACCTTTCCGTCGGT***GCT***TTCAACGGTGGCGGTG
			Y28A-Rp	CACCGCCACCGTTGAA***AGC***ACCGACGGAAAGGTAAG
2	D151N	*Sp*ChiD-WT	D151N-Fp	GACGGCATCGATCTC***AAC***TGGGAATACCCGG
			D151N-Rp	CCGGGTATTCCCA***GTT***GAGATCGATGCCGTC
3	E153Q	*Sp*ChiD-WT	E153Q-Fp	CATCGATCTCGACTGG***CAG***TACCCGGTTAACGGTG
			E153Q-Rp	CACCGTTAACCGGGTA***CTG***CCAGTCGAGATCGATG
4	Y222A	*Sp*ChiD-WT	Y222A-Fp	CCTCGATTACATCAACCTGATGACT***GCC***GATATGGCGTACG
			Y222A-Rp	CGTACGCCATATC***GGC***AGTCATCAGGTTGATGTAATCGAGG
5	Y226A	*Sp*ChiD-WT	Y226A-Fp	GATGACTTACGATATGGCG***GCC***GGCACCCAATACTTCAAC
			Y226A-Rp	GTTGAAGTATTGGGTGCC***GGC***CGCCATATCGTAAGTCATC
6	Y226W	*Sp*ChiD-WT	Y226W-Fp	CCTGATGACTTACGATATGGCG***TGG***GGCACCCAATACTTC
			Y226W-Rp	GAAGTATTGGGTGCC***CCA***CGCCATATCGTAAGTCATCAGG
7	D151N/Y28A	D151N	Y28A-Fp	CTTACCTTTCCGTCGGT***GCT***TTCAACGGTGGCGGTG
			Y28A-Rp	CACCGCCACCGTTGAA***AGC***ACCGACGGAAAGGTAAG
8	D151N/Y222A	D151N	Y222A-Fp	CCTCGATTACATCAACCTGATGACT***GCC***GATATGGCGTACG
			Y222A-Rp	CGTACGCCATATC***GGC***AGTCATCAGGTTGATGTAATCGAGG
9	D151N/Y226W	D151N	Y226W-Fp	CCTGATGACTTACGATATGGCG***TGG***GGCACCCAATACTTC
			Y226W-Rp	GAAGTATTGGGTGCC***CCA***CGCCATATCGTAAGTCATCAGG
10	D151N/Y226W/Y28A	D151N/Y226W	Y28A-Fp	CTTACCTTTCCGTCGGT***GCT***TTCAACGGTGGCGGTG
			Y28A-Rp	CACCGCCACCGTTGAA***AGC***ACCGACGGAAAGGTAAG
11	D151N/Y226W/Y222A	D151N	Y222A/Y226W-Fp	CAACCTGATGACT***GCC***GATATGGCG***TGG***GGCACCCAATACT
			Y222A/Y226W-Rp	AGTATTGGGTGCC***CCA***CGCCATATC***GGC***AGTCATCAGGTTG
12	D151N/Y28A/Y222A	D151N/Y222A	Y28A-Fp	CTTACCTTTCCGTCGGT***GCT***TTCAACGGTGGCGGTG
			Y28A-Rp	CACCGCCACCGTTGAA***AGC***ACCGACGGAAAGGTAAG
		***Sm*ChiA Mutants**		
13	D313N/F396W/Y163A	D313N/F396W	Y163A-Fp	GCAAAGTGGTCGGTTCT***GCT***TTCGTCGAGTGGGGCG
			Y163A-Rp	CGCCCCACTCGACGAA***AGC***AGAACCGACCACTTTGC
14	D313N/F396W/Y390F	D313N/F396W	Y390F-Fp	CATCTTCCTGATGAGC***TTC***GACTTCTATGGCGC
			Y390F-Rp	GCGCCATAGAAGTC***GAA***GCTCATCAGGAAGATG

Crystallization –

A catalytically inactive mutant of *Sp*ChiD, E153Q, was purified and incubated at various concentrations (12, 15 and 18 mg/mL) with 3 mM of $(GlcNAc)_6$ at 4 °C, respectively, overnight, to ensure a complete binding. These preformed complexes were used for vapour-diffusion crystallization screening in 96-well sitting drop trays, using a Mosquito crystallization robot (TTP Labtech, UK) and commercially available screens. Crystals appeared in several conditions of the JCSG-*plus*^{TM} (MD1-37) screen, and well diffracting crystals appeared by equilibrium against 0.2 M magnesium chloride, 0.1 M Tris-HCl pH 7.0 and 10% (w/v) PEG 8000 as precipitant.

Diffraction data collection, structure determination and model refinement –

Crystals were flash frozen in liquid nitrogen after a short soak in reservoir solution supplemented with 20% ethylene glycol. X-ray diffraction data of *Sp*ChiD-E153Q crystals co-crystallized with $(GlcNAc)_6$ were collected at the ID30A-1 "Massif" beamline at the European Synchrotron Radiation Facility (ESRF), in Grenoble, France. The data was integrated, scaled and analyzed using XDS[30], Aimless[31] and CCP4i[32]. The structure was solved by molecular replacement with the Phaser module in the PHENIX software[33], using the structure of the ligand-free *Sp*ChiD as a search model (4NZC.pdb)[34]. The refinement was done using PHENIX[33] and each refinement cycle was interspersed with rebuilding and manual adjustments using Coot[35]. The asymmetric unit of the final model contains 2 protein chains of 399 and 398 residues, respectively, as well as 2 $(GlcNAc)_2$ molecules, 4 ethylene glycol molecules, 2 chloride ions and 995 solvent water molecules. A few side chains have been modeled with two alternative conformations. A simulated annealing composite-omit map was calculated using PHENIX,[33] omitting 5% of the model for each map, to verify the density of the modeled chitobiose (Fig 3C). Final atomic coordinates and structure factors have been deposited in the Protein Data Bank with accession code 6F8N.

Product analysis by UPLC –

Chitin mono- and oligosaccharides were purchased from Megazyme (Wicklow, Ireland). Quantitative analysis of $(GlcNAc)_{1\text{-}6}$ was performed using a long hydrophilic interaction chromatography (HILIC) column (Acquity UPLC BEH Amide, 300Å, 1.7 μm, 2.1 mm × 150 mm) as described previously[36] with minor modifications. The sample injection volume was 7.0 μL and the flow rate was maintained as 0.4 mL/min. The gradient was as follows: The starting conditions, 20% eluent A (15 mM Tris–HCl pH 8.0), 80% eluent B (100% acetonitrile) were held for 5 min,

followed by a 7 min linear gradient to 70% B and a 4 min linear gradient to 55% B. Column reconditioning was obtained by a 2 min gradient back to initial conditions (20% A: 80% B), which were then held for 4 min. Products were detected by monitoring absorbance at either 195 nm or 205 nm. At 205 nm the signal-to-noise ratio is better and peak integration is more accurate and therefore the absorbance values at 205 nm were considered for product quantification. A linear correlation between peak area and concentration of each $(GlcNAc)_n$ in standard samples was established for quantification of $(GlcNAc)_{1-6}$ oligomers. Standard calibration curves for $(GlcNAc)_{1-6}$ were constructed separately. These data points yielded a linear curve for each standard sugar with R^2 values of 0.997 – 1.0, allowing the molar concentrations of $(GlcNAc)_{1-6}$ to be determined with confidence.

Specific activity measurements and TG assay with $(GlcNAc)_4$ as substrate –

For determination of the initial rates of *Sp*ChiD variants, reaction mixtures contained 0.6 mM $(GlcNAc)_4$ in 20 mM Tris-HCl, pH 8.0, and the enzyme concentration was adapted to the activity of the tested variant (0.1 μM − 1 μM). For monitoring of TG activity of *Sp*ChiD variants, reactions were set up with 0.6 mM $(GlcNAc)_4$ as the substrate and 1.0 μM of enzyme, in 20 mM Tris-HCl, pH 8.0. The properties of *Sm*ChiA variants were assessed in a similar manner, using 1.0 mM $(GlcNAc)_4$ and 3.0 μM of enzyme in 20 mM ammonium acetate, pH 6.1, containing 0.1 mg/mL BSA, for determination of both initial rate and TG activity. For determination of the initial rate for wild-type *Sm*ChiA, the enzyme concentration was 10 nM. All reactions were performed at 37 °C.

Fractions were collected at regular time intervals and the reaction was stopped by adding an equal volume of 100% acetonitrile and samples were stored at −20 °C until UPLC analysis of reaction products, as described above. All the reactions were run in triplicate. When determining initial rates for specific activity measurements, care was taken to have true initial conditions, meaning that the rate of hydrolysis of $(GlcNAc)_4$ was constant over time and that the $(GlcNAc)_4$ concentration always remained above 80% of the starting concentration.

The TG potential was assessed in a qualitative manner by quantifying all TG products over time for reactions that were run until most of the substrate had been consumed. For *Sp*ChiD $(GlcNAc)_5$ and $(GlcNAc)_6$ were monitored, whereas for *Sm*ChiA, with its higher hydrolytic activity on compounds like $(GlcNAc)_5$ and $(GlcNAc)_6$, formation of $(GlcNAc)_3$ was monitored. *Sm*ChiA cannot directly convert $(GlcNAc)_4$ to GlcNAc and $(GlcNAc)_3$ meaning that $(GlcNAc)_3$

can only emerge as a result of hydrolysis of longer oligomers that were generated in a preceding TG event.[12]

Results

Residue analysis and mutant design –

Comparison of amino acid sequences pertaining to the catalytic domains of family 18 chitinases of different origin (bacterial eg. *Sp*ChiD, *Sm*ChiA, *Sm*ChiB, *B*cChiA1 and plant eg. chitinase from *Cycas revoluta* (*Cr*Chi)) through structure based sequence alignment (Fig. 1) revealed the presence of strictly conserved and also similar residues that were shown to be important for either hydrolysis or TG activity. Previous studies of GH18 chitinases had indicated that TG activity may be obtained by increasing the hydrophobicity/binding surface area of acceptor subsites (+ subsites) or by mutating residues important for stabilizing the oxazolinium ion intermediate ("catalytic residues"). In the current work, we chose to study additional residues that has been shown to be important for catalysis and intermediate stabilization for a GH18 chitinase (*Sm*ChiB) through biochemical assays, computational analyses, and crystal structures of complexes with different carbohydrate ligands.[20,21]

D149, D151, and E153 (*Sp*ChiD numbering) in the conserved DXDXE motif, are key catalytic residues, where E153 is the catalytic acid. These residues are situated on a TIM-barrel β-strand with E153 on the top (Fig. 2A; Fig. 3). Prior to substrate binding, D151 is rotated down in the barrel making a hydrogen bond to D149. When substrate binds, this hydrogen bond is broken and D151 rotates upwards, now making hydrogen bonds with the catalytic acid, E153, and the NH of the *N*-acetyl-group of the sugar bound in the -1 subsite, which becomes positively charged in the oxazolinium ion intermediate. D151 in *Sp*ChiD corresponds to D313 in *Sm*ChiA (Fig. 2B; the large difference in sequence number is due to the presence of an N-terminal FnIII domain in *Sm*ChiA only). From earlier work[12], it was known that mutation of D151 to asparagine may be beneficial for TG activity.

Several other residues contribute to intermediate formation and stabilization. Y28 in *Sp*ChiD (Y163 in *Sm*ChiA) is situated in the –1 subsite (Fig. 2 & 3) and the methyl group of the *N*-acetyl-group of the –1 sugar has a hydrophobic stacking interaction with the benzene ring of the tyrosine. Moreover, studies of *Sm*ChiB have shown that, upon substrate binding, this tyrosine shifts by up to 2 Å, placing its phenolic hydroxyl group at 2.6 Å from D149 which compensates for the

temporary loss of hydrogen bonding interactions due to the rotation of its hydrogen bonding partner, D151, towards E153. Another tyrosine, Y222 in *Sp*ChiD (Y390 in *Sm*ChiA) seems to be of particular importance for interactions with the intermediate since, upon substrate binding, the hydroxyl group of this tyrosine forms a hydrogen bond with the carbonyl oxygen of the *N*-acetyl-group of the –1 sugar This interaction helps positioning the *N*-acetyl group for nucleophilic attack on the anomeric carbon and is likely maintained in the oxazolinium ion intermediate. Both Y28 and Y222 (*Sp*ChiD numbering) were targeted for mutagenesis.

The final residue targeted in this study was Y226 (F396 in *Sm*ChiA) which is situated in the +2 subsite (Fig. 2 & 3). Substrate binding creates a hydrophobic interaction between the aromatic amino acid and the +2 sugar moiety and it had been shown previously that replacing F396 in *Sm*ChiA by tryptophan was beneficial for TG activity[12]. Notably, W114 (W275 in *Sm*ChiA), making a seemingly strong stacking interaction with the substrate in subsite +1 (Fig. 3), was not mutated since this residue has shown to promote TG activity in several family 18 chitinases.[12, 14, 26]

When constructing new mutants, we chose to keep the Asp to Asn mutation at the 151- (*Sp*ChiD) and 313- (*Sm*ChiA) position. The mutation to Asn is the only "clean" mutation that removes the crucial charge in position 151, without any further sterical effects and likely with little effects on hydrogen bonding. The effect of e.g. the D151Q mutation would be more unpredictable. In positions 28 (*Sp*ChiD) and 163 (*Sm*ChiA) 222 (*Sp*ChiD) and 390 (*Sm*ChiA) a Tyr was exchanged with an Ala residue to i) remove a stabilizing interaction of the intermediate, ii) introduce hydrophobicity, and iii) chose a residue that is generally considered to result in a safe exchange. Introduction of Y390A in *Sm*ChiA was successful, but resulted in poor protein production. Instead, Y390F was chosen as Phe resembles Tyr in size, but is incapable to participate in a hydrogen bond with the intermediate. *Sm*ChiA-Y390F could be produced in sufficient amounts for enzyme characterization with respect to TG activity.

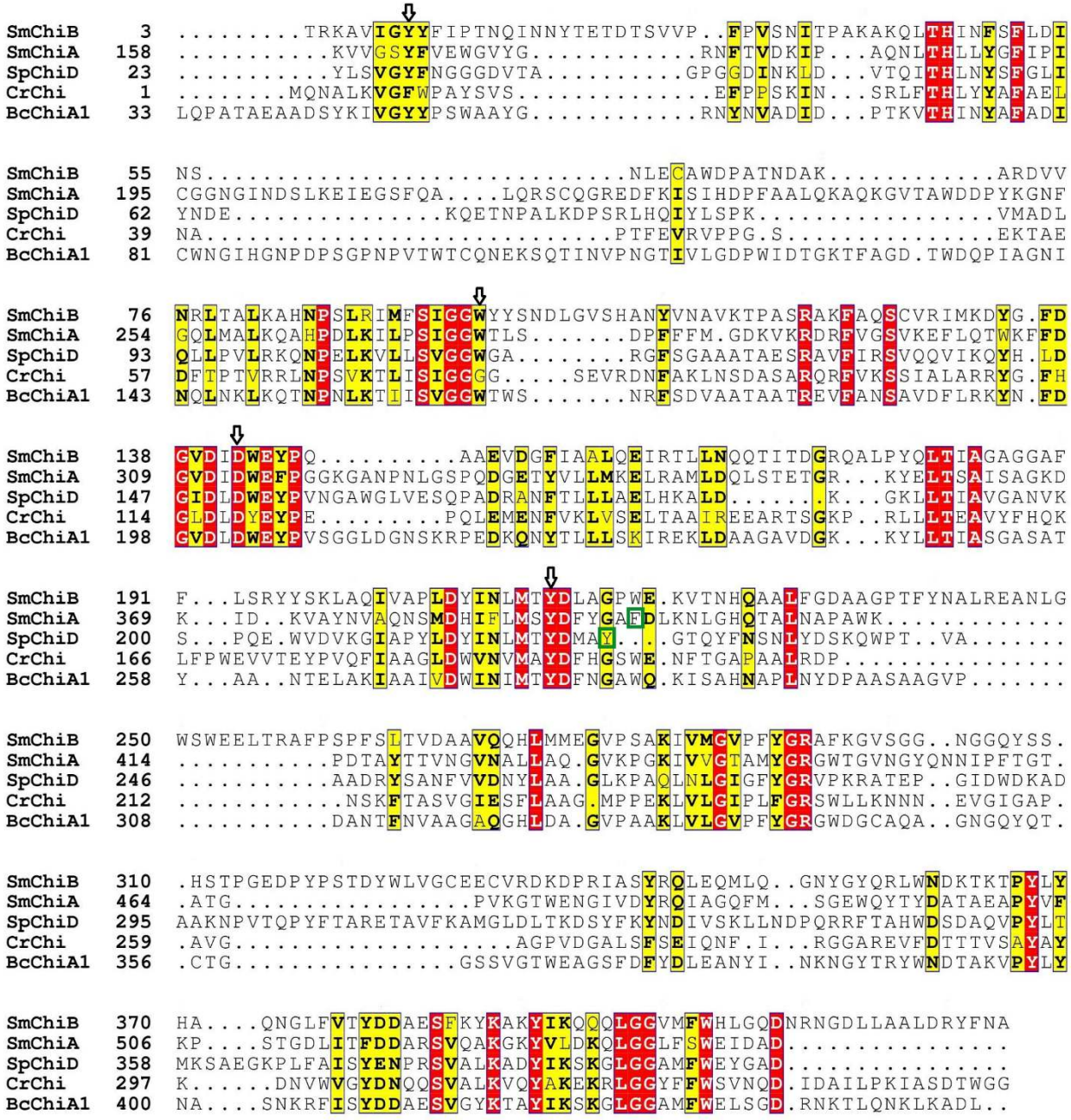

Figure 1. Structure based sequence alignment was created by considering the amino acid sequence corresponding to the catalytic domains of *Sp*ChiD (4NZC), *Sm*ChiA (1EDQ), *Sm*ChiB (1E15), *Cr*Chi (4MNJ) and *Bc*ChiA1 (1ITX). Similar residues are shown in black bold characters and boxed in yellow, while, the strictly conserved residues are shown as white characters on a red background. Arrows and/or characters shown in green boxes indicate the residues that are examined or discussed in the current study.

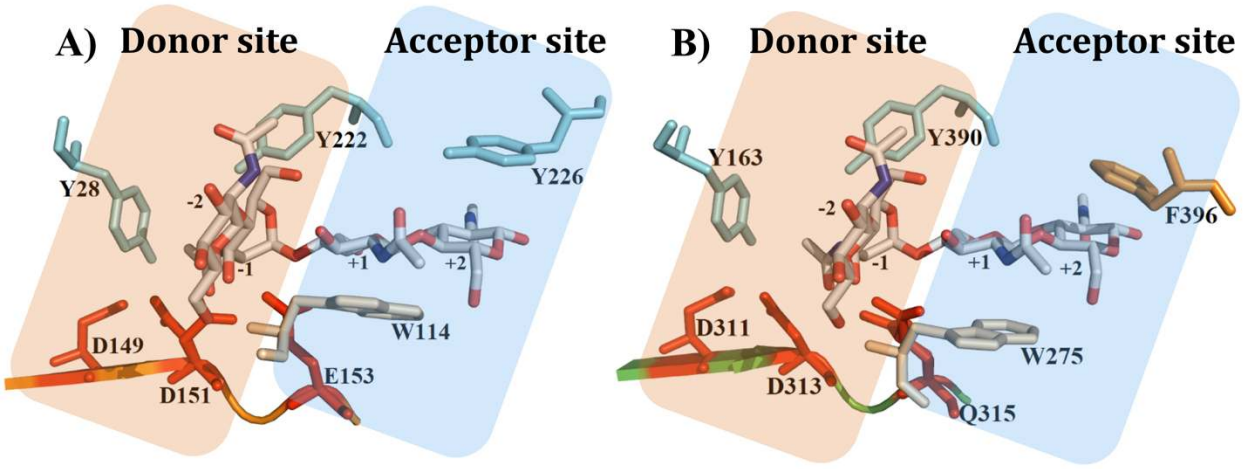

Figure 2. Schematic representation of the key residues interacting with the $(GlcNAc)_4$ from donor and acceptor subsites of *Sp*ChiD (A) and *Sm*ChiA (B). The crystal structures of *Sp*ChiD (PDB: 4NZC) and *Sm*ChiA (PDB: 1NH6) were used for representing the respective substrate-binding clefts. The side chains of key residues affecting TG activity are shown as sticks and the catalytic residues of both the enzymes are shown as red color sticks. The co-ordinates of $(GlcNAc)_4$ were taken from the PDB: 1NH6 and only four of the seven GlcNAc units are shown in sticks occupying the subsites −2 to +2 and the nitrogen atoms are colored dark blue, and oxygen atoms are colored red.

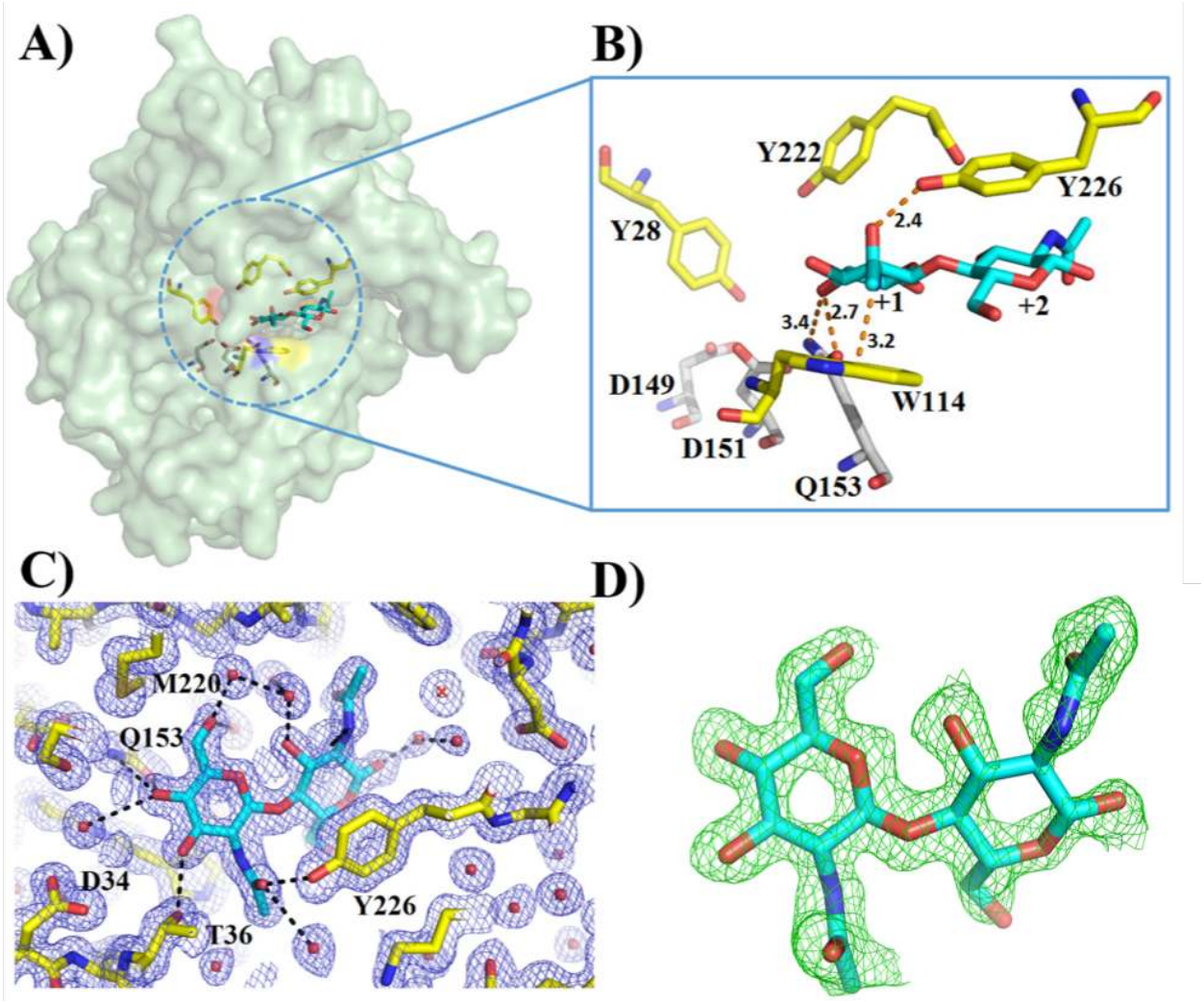

Figure 3. **Crystal structure of *Sp*ChiD_E153Q in complex with $(GlcNAc)_2$**. (A) Surface representation showing the sides chains of key residues (yellow carbons) important for chitinase activity and binding of a $(GlcNAc)_2$ molecule that occupies subsites +1 and +2 (blue carbons). (B) Close-up view of selected residues and their interactions with $(GlcNAc)_2$; potential interactions are shown as dashed lines with distances in Å. Residue 153 is the catalytic acid/base which was mutated from glutamate to glutamine. C) 2Fo-Fc electron density map for chitobiose and active site of *Sp*ChiD contoured at 1.0 sigma level. Selected interactions between the chitobiose and nearby solvent water molecules and enzyme residues are shown as dashed lines. (D) Simulated annealing composite omit map around the chitobiose. Map contoured at 1.0 sigma level.

Crystal structure of *Sp*ChiD-E153Q in complex with $(GlcNAc)_2$ –

A crystal structure determination study was undertaken to confirm that the intermolecular interactions observed between a (GlcNAc) oligomeric substrate and *Sm*ChiB and *Sm*ChiA, respectively, also are formed in *Sp*ChiD. A crystal of *Sp*ChiD-E153Q in complex with a ligand was obtained by incubation of the protein with $(GlcNAc)_6$ prior to crystal screening. The structure was determined at a resolution of 1.45 Å (Table 2) and revealed the presence of a chitobiose molecule bound to subsites +1 and +2 (Fig. 3). The chitobiose is likely a product generated by the mutant, which probably retains a very low catalytic activity. A residual catalytic activity of 0.024 % of the wild type has previously been observed for *Sm*ChiB-E144Q (corresponding mutation)[21]. It is likely that the combination of (i) the ability of the protein to distort the -1 sugar to a boat conformation (i.e. as observed in van Aalten *et al.* (2001)[20], Perrakis *et al.* (1994)[37]), which is required for hydrolysis, (ii) the presence of water in the active site as shown in the crystal structure (Fig. 3C), and (iii) the long incubation time of the crystallization experiments, is sufficient for hydrolysis to take place. Chen *et al*. (2014) have previously observed similar occurrence.[38] The presence of the chitobiose molecule is likely due to a relative strong binding interaction with *Sp*ChiD, which was reported to have a K_a of 4.22×10^4 M^{-1} (K_d = 0.24 mM and $\Delta G°$ = –6.0 kcal/mol).[14] In a different example, this binding interaction has been determined to yield K_a of 2.5×10^3 M^{-1} (K_d = 0.40 mM and $\Delta G°$ = –4.6 kcal/mol) for *Sm*ChiA.[39] The structure of *Sp*ChiD-E153Q was highly similar to that of wild-type *Sp*ChiD[34], with an r.m.s. deviation of less than 0.2 Å for a superposition of 2695 protein atoms. Fig. 3B shows that the pyranose rings of the +1 and +2 sugar residues stack against the side chains of W114 and Y226, respectively.

Table 2. Crystal data, data-collection statistics and refinement data.

Data Collection	
Beamline	ID30A-1 (ESRF, Grenoble)
Wavelength (Å)	0.96600
Temperature (K)	100
Space Group	*C*2
Unit-cell parameters (Å, °)	a=128.84, b=87.57, c=75.39
	$\alpha = \gamma = 90$; $\beta = 115.5$
Resolution (Å)	69.96 - 1.45 (1.47 - 1.45)[a]
Unique reflections	126 010 (4074)
Completeness (%)	93.9 (60.6)
Multiplicity	2.8 (1.9)
Mean I/σI	9.9 (2.1)
R_{merge} (all I^+ and I^-)	0.063 (0.325)
Refinement statistics	
Resolution of data used in refinement	69.96 – 1.45
Completeness for range (%)	93.9
R_{cryst}/R_{free} (%)[b]	17.5/20.9
R.m.s.d. bonds (Å)	0.006
R.m.s.d. angles (°)	0.85
Average B-factor (protein/solvent/NAG ligand) (Å^2)	17.7 / 29.6 / 22.8
Number of atoms in model	
Protein	6261
Solvent waters	995
Chitobiose ligands	58
Ethylene glycol	16
Chloride ions (Cl^-)	2
Ramachandran plot (%) [c]	
Favorable region	97.5
Additionally allowed	2.5

[a] Values in parentheses are for the highest resolution shells

[b] $R_{cryst} = \Sigma_{hkl} |F_o - F_c| / \Sigma_{hkl} |F_o|$ where F_o and F_c are the observed and calculated structure factor amplitudes, respectively. R_{free} is calculated from a randomly chosen 4.92% set of unique reflections not used in refinement.

[c] Defined using MolProbity[40].

Table 3. Specific activity and relative TG activity of *Sp*ChiD and *Sm*ChiA variants, when acting on $(GlcNAc)_4$ as the substrate.

Enzyme[1)]	Specific activity µmol.s^{-1}.mg^{-1}	% of wild type	Relative TG activity[2)]	Percentage TG Activity[3)]
***Sp*ChiD**	202 ± 12	100	+	11
Y28A	216 ± 19	107	++	21
Y222A	232 ± 11	115	++	21
Y226A	142 ± 6	70	─	─
Y226W	40 ± 4	20	+	15
D151N	1.2 ± 0.3	0.6	++	19
D151N/Y28A	0.7 ± 0.1	0.3	++	15
D151N/Y222A	1.5 ± 0.1	0.7	+++	22
D151N/Y226W	1.1 ± 0.2	0.6	+++	22
D151N/Y226W/Y28A	0.4 ± 0.1	0.2	++	17
D151N/Y226W/Y222A	1.5 ± 0.1	0.8	++++	>22
D151N/Y28A/Y222A	─	─	─	
***Sm*ChiA**	708 ± 44	100	+	
D313N/F396W	1.6 ± 0.1	0.2	++	
D313N/F396W/Y163A	1.3 ± 0.1	0.2	+++	
D313N/F396W/Y390F	3.0 ± 0.1	0.4	++++	

1) Analogous residues in *Sp*ChiD and *Sm*ChiA have different numbers. The corresponding numbers are (*Sp*ChiD first): 28-163; 151-313; 222-390; 226-396.
2) TG activity of *Sp*ChiD variants was scored based on visual inspection of the progress curves of Figures 5B, 5C, 6B and 6C, whereas TG activity of *Sm*ChiA variants was scored based on visual inspection of the progress curves of Figure 7C. Scoring was based on +: activity of the wild types ("minimal activity"), ++++: highest activity observed for a constructed mutant ("very high activity); ++ and +++: intermediate activity relative to that observed for the wild types and highest activity. ─: no activity.
3) Estimates of oxazolinium ion intermediates undergoing TG reactions as explained in the manuscript text.

Specific hydrolytic activity of the *Sp*ChiD and *Sm*ChiA variants –

Specific hydrolytic activities against $(GlcNAc)_4$ were measured by monitoring the initial rate of substrate disappearance and Table 3 shows the results for all enzyme variants assessed in this study. The activity of mutants *Sp*ChiD-Y28A and *Sp*ChiD-Y222A was similar to, or perhaps slightly increased, compared to the wild-type. *Sp*ChiD-Y226W and *Sp*ChiD-Y226A showed a 30 % and 80 % decrease in specific activity, respectively, and, as expected, the *Sp*ChiD-D151N variant displayed the greatest reduction in activity of all the single mutants (1 % of wild-type activity). All *Sp*ChiD variants with multiple mutations contained the D151N mutation and showed specific activities in the range of 1 % of the wild-type, except for the triple mutant *Sp*ChiD-D151N/Y28A/Y222A, for which hydrolytic activity could not be detected. As observed for *Sp*ChiD, the different *Sm*ChiA variants, which all contained the D313N mutation analogous to D151N in *Sp*ChiD, showed similar specific activities as the single mutant *Sm*ChiA-D313N. Notably, we were not able to produce sufficient protein amounts for *Sp*ChiD variants in which Y222 (analogous to Y390 in *Sm*ChiA) had been mutated to phenylalanine.

TG activity of *Sp*ChiD variants –

Effect of single mutants –

The impact of mutations on TG activity of *Sp*ChiD was studied by monitoring product formation over time in reactions with $(GlcNAc)_4$ as the substrate. HPLC analysis of product mixtures showed that wild-type *Sp*ChiD and its mutants generated a mixture of oligosaccharides, *i.e.* $(GlcNAc)_{1\text{-}8,}$ even in the very beginning of the reaction. The TG potential of all the mutants was compared by considering the production of $(GlcNAc)_5$ and $(GlcNAc)_6$, as determined by HPLC analysis of product mixtures. TG products beyond $(GlcNAc)_6$ were not quantified due to the lack of standards. Hereafter, $(GlcNAc)_{5,6}$ will be referred as quantifiable TG products. In Fig. 4, a schematic possible transglycosylation reaction for *Sp*ChiD is depicted using $(GlcNAc)_4$ as substrate. Fig. 5 shows results for the single mutants, all of which, except D151N, gave an expected rapid decrease in the initial substrate concentration (Fig. 5A).

The *Sp*ChiD-Y226A showed very little TG activity, which was to be expected since it is known from other mutagenesis studies of GH18s that an aromatic residue in this position is beneficial for TG.[12, 25] All other single mutants showed increased TG activity compared to the wild type. Whereas, the wild-type and *Sp*ChiD-Y226W showed an early peak of TG products that

rapidly disappeared due to hydrolysis, TG products generated by the other single mutants were more persistent. Interestingly, the *Sp*ChiD variants showed clear differences in the product patterns. Looking at peak levels $(GlcNAc)_5$ and $(GlcNAc)_6$, we see that *Sp*ChiD-Y222A catalyzed the formation of 80 μM of $(GlcNAc)_5$ and 45 μM of $(GlcNAc)_6$ adding up to 125 μM in total (Fig. 5B & 5C). The starting concentration of $(GlcNAc)_4$ was 600 μM indicating that 21 % of available oxazolinium ion intermediates undergoes TG reactions (21 % TG activity). Since the formation of 125 μM TG products requires the consumption of 250 μM of the starting substrate $(GlcNAc)_4$ (see Fig. 4), a percentage of $(GlcNAc)_4$ involved in TG formation of 42 % can be estimated. Both numbers must be viewed as estimates since $(GlcNAc)_5$ and $(GlcNAc)_6$ also are substrates for subsequent hydrolysis and TG reactions. *Sp*ChiD-Y28A generated 75 μM $(GlcNAc)_6$ and 50 μM $(GlcNAc)_5$, also adding up to 125 μM in total (21 % TG activity).

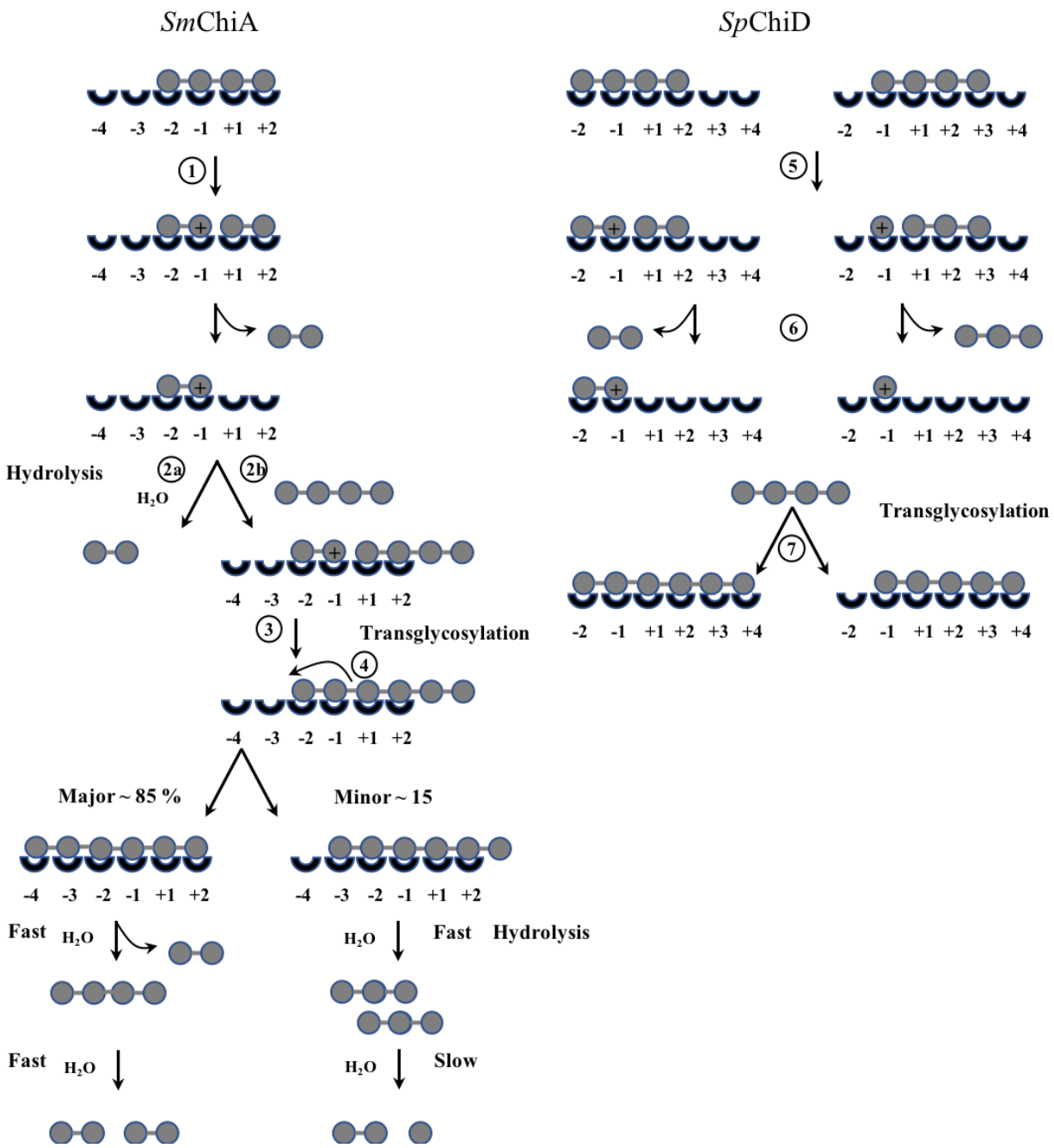

Figure 4. Schematic depiction of possible transglycosylation reaction using $(GlcNAc)_4$ as substrate. GlcNAc residues are shown as gray circles, and the binding subsites of the enzyme are numbered. For *Sm*ChiA, the $(GlcNAc)_4$ substrate binds to the –2 to +2 subsites, and the glycosidic bond is cleaved to form a positive charged "$(GlcNAc)_2$" oxazolinium ion intermediate (marked with +) in the –1 and –2 subsites (step 1). A $(GlcNAc)_2$ product then exits and is replaced by an incoming water (step 2a) or acceptor $(GlcNAc)_4$ (step 2b). In the second case (transglycosylation), a $(GlcNAc)_6$ is formed (–2 to "+4") (step 3). This transglycosylation product is released and may after rebinding (step 4) be subjected to hydrolysis or further transglycosylation reactions. In the

event of hydrolysis, all subsequent reactions are fast except for $(GlcNAc)_3$, which accumulates and only occurs if a transglycosylation reaction has taken place allowing a quantification of TG activity. For *Sp*ChiD, the $(GlcNAc)_4$ substrate binds to either –2 to +2 subsites or –1 to +3 subsites, and the glycosidic bond is cleaved to form a positive charged "$(GlcNAc)_2$" or "(GlcNAc)" oxazolinium ion intermediate in the –1 and –2 subsites or –1 subsite (step 5). A $(GlcNAc)_2$ or $(GlcNAc)_3$ product then exits and replaced an i.e. acceptor $(GlcNAc)_4$ to produce $(GlcNAc)_6$ and $(GlcNAc)_5$, respectively, allowing a quantification of TG activity.

As expected, *Sp*ChiD-D151N reacted much more slowly ending up at peak levels of 75 μM of $(GlcNAc)_5$ and 45 μM of $(GlcNAc)_6$ adding up to 115 μM in total (19 % TG activity) (Fig. 5B & 5C). Due to the slow hydrolytic activity of this variant, the levels TG kept increasing or at least remained stable during the full 24 hours of the reaction. The *Sp*ChiD-Y226W variant produced up to 45 μM of both $(GlcNAc)_5$ and $(GlcNAc)_6$ (90 μM in total, 15 % TG activity), which is higher compared to the wild-type (37 and 30 μM, respectively, 11 % TG activity) (Fig. 5B & 5C). The differences in $(GlcNAc)_5$ and $(GlcNAc)_6$ concentrations likely reflect changes in binding preferences in individual subsites caused by the mutations due to the contribution of the original residues have on the binding free energy to the substrate versus the new residues. An example of this is when W167 in subsite –3 in *Sm*ChiA, which provides 2 kcal/mol in binding free energy to the sugar moiety in this subsite[41], is exchanged to alanine, the preference for productive binding of $(GlcNAc)_5$ is shifted from being equal between subsites –3 to +2 and to –2 to +3 to be about 90 % in favor of binding from subsites –2 to +3.[42]

Effect of double and triple mutants –

Since the equivalent the D151N mutation has shown to be a key factor for TG activity for several family 18 chitinases and since *Sp*ChiD-D151N was superior among the single mutants in terms to maintaining a high concentration of TG products, we combined single mutations with beneficial effects on TG activity with D151N. All multiple mutants showed TG activity, with roughly similar $(GlcNAc)_5$:$(GlcNAc)_6$ ratios and very good product stability, but with considerable variation in the rate of TG product accumulation, which correlated with variation in the initial rate of substrate disappearance (Fig. 6). The two mutants containing Y28A, *Sp*ChiD-D151N/Y28A and D151N/Y226W/Y28A showed total TG product levels of 90 μM and 100 μM after 24 hours (15 % and 17 % TG activity, respectively), but in this case, the reactions did not seem finished. The other mutants displayed slightly higher total TG product levels, over 130 μM (over 22 % TG activity)

(Fig. 6B & 6C). The *Sp*ChiD-D151N/Y226W/Y222A stood out by accumulating high levels of TG products early in the reaction (Fig. 6B & 6C, orange curves). Notably, for this mutant, the apparent consumption of $(GlcNAc)_4$ stopped after the levels of $(GlcNAc)_5$ and $(GlcNAc)_6$ had reached the maximum, which suggests that the reaction enters some sort of stable equilibrium, where consumption and production (from degradation of longer TG products) of $(GlcNAc)_4$ are balanced. This suggest that *Sp*ChiD-D151N/Y226W/Y222A is highly suitable for carrying out TG reactions.

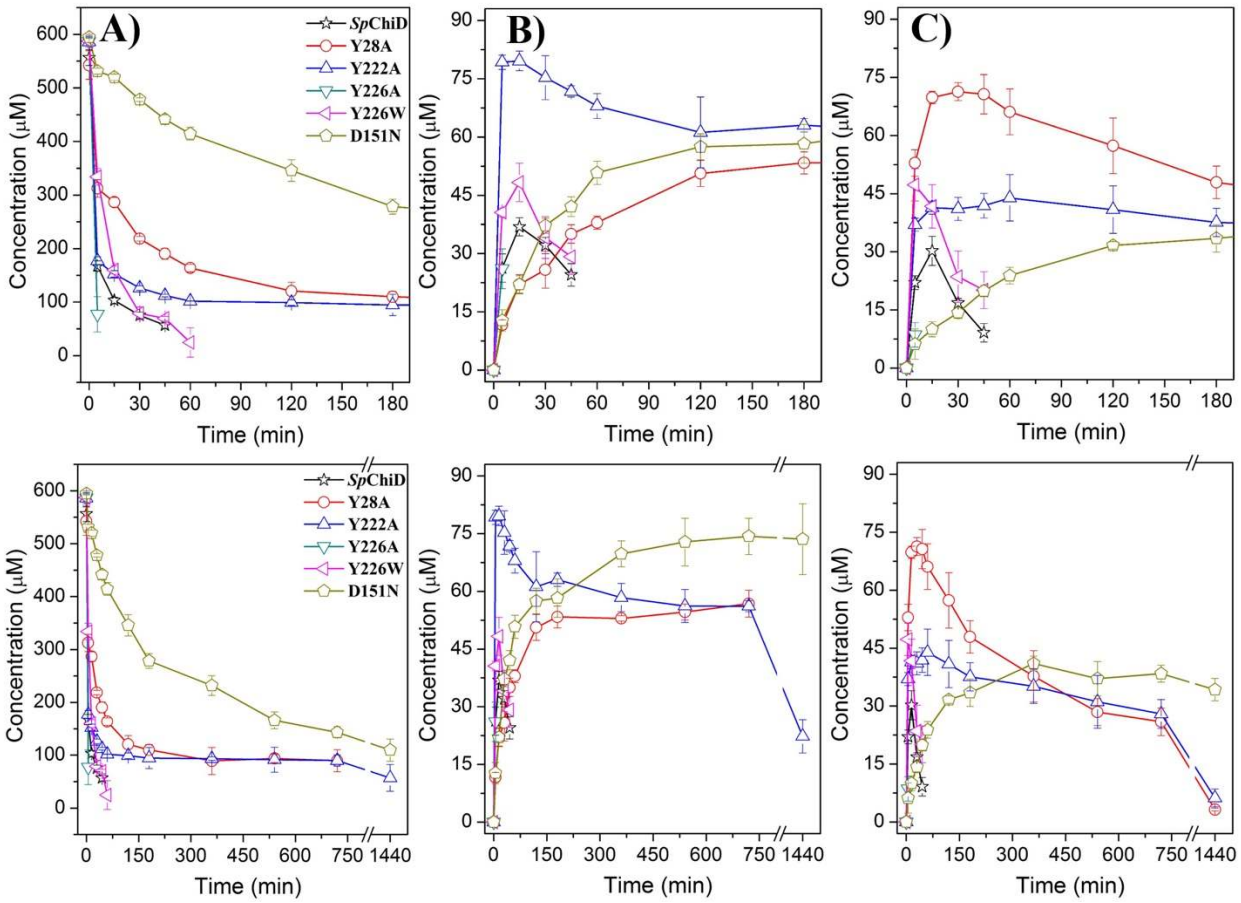

Figure 5. Product formation by *Sp*ChiD and its single mutants. The plots show the concentration of the substrate, $(GlcNAc)_4$ (A) and of the quantifiable TG products $(GlcNAc)_5$ (B) and $(GlcNAc)_6$ (C). For a clear view, the data points pertaining to the initial phase of reaction (0 – 180 min) are shown separately in the upper panel of the figure, while the lower panel includes complete set of data points for each mutant measured up to 24 h. The reaction mixtures contained 0.6 mM $(GlcNAc)_4$ and 1μM of each enzyme in 20 mM Tris-HCl, pH 8.0 and were incubated at 37 °C. The error bars represent the standard deviations from three individual experiments.

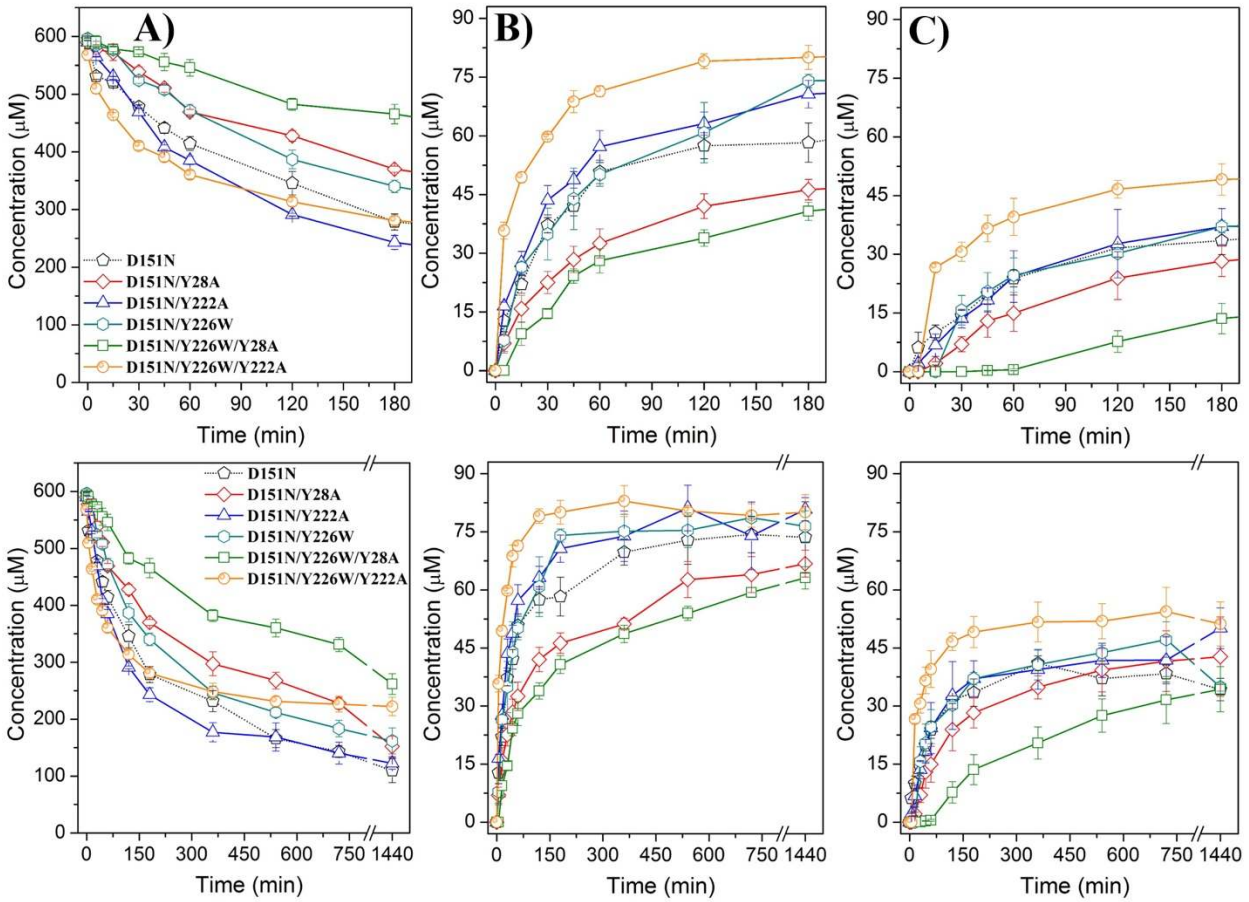

Figure 6. Product formation by *Sp*ChiD multiple mutants. The plots show the concentration of the substrate, $(GlcNAc)_4$ (A) and of the quantifiable TG products $(GlcNAc)_5$ (B) and $(GlcNAc)_6$ (C). For a clear view, the data points pertaining to the initial phase of reaction (0 – 180 min) are shown separately in the upper panel of the figure, while the lower panel includes complete set of data points for each mutant measured up to 24 h. The reaction mixtures contained 0.6 mM $(GlcNAc)_4$ and 1μM of each enzyme in 20 mM Tris-HCl, pH 8.0 and were incubated at 37 °C. The error bars represent the standard deviations from three individual experiments.

TG activity of *Sm*ChiA variants –

*Sm*ChiA-D313N/F396W, a previously described variant of *Sm*ChiA with improved TG activity[12] that is analogous to *Sp*ChiD-D151N/Y226W, was used as a template to see if mutations showing a positive effect on TG activity in *Sp*ChiD had the same effect in *Sm*ChiA, and to see if the combination of such residues would give an additive effect. Thus, triple mutants D313N/F396W/Y163A (Y163 analogous to Y28 in *Sp*ChiD) and D313N/F396W/Y390F (Y390 analogous to Y226 in *Sp*ChiD) were generated. In the case of *Sm*ChiA, longer TG products are too

susceptible to hydrolysis to be observed and TG activity is quantified by measuring the level of $(GlcNAc)_3$, a product that can only be generated from a previously generated TG product with a degree of polymerization > 4 (Fig. 4).[12] For this reason, percentage TG activity was not estimated for *Sm*ChiA mutants.

Compared to the starting variant, both triple mutants showed slightly reduced catalytic rates (as evident from the rate of disappearance of $(GlcNAc)_4$ or production of $(GlcNAc)_2$; Fig. 7A & 7B), and increased TG activity, as reflected in increased production of $(GlcNAc)_3$ (Fig. 7C). Very interestingly, the *Sm*ChiA-D313N/F396W/Y390F showed the clearly best TG performance, as reflected by a steadily increasing level of $(GlcNAc)_3$ throughout the reaction, reaching 140 μM after 24 hours (Fig. 7C). As such, this mutant is quite similar to the best performing mutant of the *Sp*ChiD, *i.e.* *Sp*ChiD-D151N/Y226W/Y222A, which carries mutations at the same three positions. Combined these results show that the residues important for TG activity in *Sp*ChiD also are important for TG activity in *Sm*ChiA.

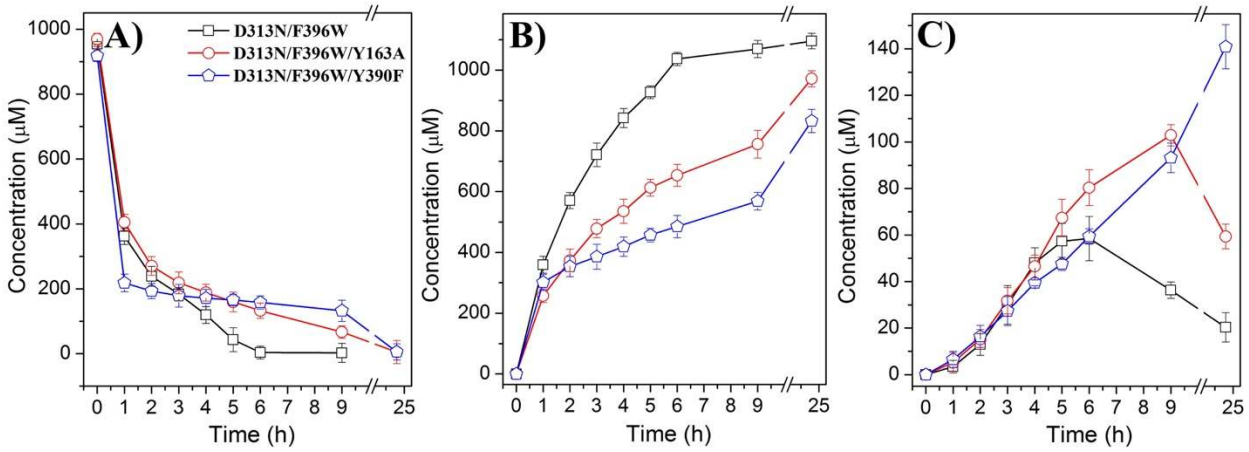

Figure 7. Product formation by *Sm*ChiA multiple mutants. The plots show the concentration of the substrate, $(GlcNAc)_4$ (A) and of the quantifiable products $(GlcNAc)_2$ (B) and $(GlcNAc)_3$ (C), where the latter is an indicator of TG activity. Wild type *Sm*ChiA produced 15 μM of $(GlcNAc)_3$, which did not accumulate beyond 3 min of reaction time. For this reason, the data are omitted from the Figure for clarity. The reaction mixtures contained 1.0 mM $(GlcNAc)_4$ and 3.0 μM of enzyme in 20 mM ammonium acetate, pH 6.1, containing 0.1 mg/mL BSA. The error bars represent the standard deviations from three individual experiments.

Discussion

In the current work, we observed that the exchange of several residues involved in catalysis by family 18 chitinases alters the yield of TG products. Moreover, the combination of mutations

yielded even higher degrees of TG activity, including mutations affecting subsite affinity and a mutation, D151N, whose primary goal was to strongly reduce but not abolish the hydrolytic activity. The latter mutation reduced the hydrolytic activity of *Sp*ChiD about 200-fold (Table 2). Previous kinetic studies with *Sm*ChiA, also using $(GlcNAc)_4$ as substrate, showed a k_{cat} of 33 s^{-1} for the wildtype versus 0.60 s^{-1} for *Sm*ChiA-D313N[12]. A common observation across families of retaining glycoside hydrolases is that increased TG activity can be obtained by decreasing the rate of hydrolysis[43]. This is obviously due in part to less efficient degradation of TG products, but also relates to the fact that residues affecting the transition state of the reaction, and, thus, the rate, also likely affect the stability, position and conformation of intermediate states.

In the mechanism for GH18 catalysis, an oxazolinium ion is a proposed intermediate that normally undergoes nucleophilic attack of a water molecule[18-20]. In 1996, Kobayashi et al.[44] showed that incubation of a chitobiose oxazolinium with a wild-type family 18 chitinase from *Bacillus* sp. resulted in the generation of CHOS with a degree of polymerization between 10 and 20. This suggests that the oxazolinium derivative has a propensity to accept a sugar molecule as the nucleophile over a water molecule. The magnitude of this propensity in cases when a chitinase is acting on a normal substrate, $(GlcNAc)_4$ in this case, is not clear. It is conceivable, however, that this propensity may be influenced by mutations that affect the stability, conformation and/or orientation of the oxazolinium ion intermediate in the catalytic center. This was the rationale behind mutating Y28 and Y222 in *Sp*ChiD, which indeed had effects on the apparent TG activity.

Y222 in the -1 subsite of *Sp*ChiD forms a hydrogen bond with the carbonyl oxygen of *N*-acetyl-group of the –1 sugar, i.e. the group that carries out nucleophilic attack on the anomeric carbon during substrate-assisted catalysis[18, 20, 21]. This hydrogen bond is likely maintained in the oxazolinium ion intermediate. Y28 has been proposed to be part of a system for dispersion of charge and displacement of protons during catalysis[21]. It is thus conceivable that mutations of these residues affect properties of the reaction intermediate that influence its susceptibility to nucleophilic attack by water versus a sugar acceptor. Notably, despite proposed roles of these residues in the catalytic mechanism, their mutation in *Sp*ChiD did not seem to change the rate of hydrolysis of $(GlcNAc)_4$. Previous studies using substrates with non-natural leaving groups such as 4-methylumbelliferyl have shown that mutations of residues analogous to Y28 and, in particular, Y222 reduce catalytic activity[21]. Here, we used a natural substrate, with a different leaving group,

which may explain the different results[45]. Furthermore, both structural[34] and activity data, such as an exceptionally high natural TG activity[13, 14], indicate that catalysis in *Sp*ChiD differs significantly from other GH18 chitinases (see below).

Next to reducing hydrolytic activity, the D151N mutation may also specifically affect the oxazolinium intermediate. In the work of Jitonnom *et al*. (2011)[46], it was shown through Quantum Mechanics/Molecular Mechanics that D142 in *Sm*ChiB (equivalent to D313 and D151 in *Sm*ChiA and *Sp*ChiD, respectively) stabilized the transition state and the oxazolinium ion intermediate to a higher extent than N142, providing a theoretical explanation for the well-known deleterious effect of the D → N mutation on hydrolytic activity. Considering the important interaction between this residue and the oxazolinium ion intermediate, it is conceivable that, compared to aspartate, an asparagine in this position stabilizes the intermediate in a state that is more susceptible for nucleophilic attack by a sugar molecule.

Our work provides further support to the importance of increasing the hydrophobicity/binding surface area in positive subsites that presumably promotes binding of an acceptor sugar molecule. The increase in hydrophobicity/binding surface area through the exchange of Y226 to tryptophan at subsite +2 in *Sp*ChiD is analogous to the similar exchange of F396 to tryptophan in *Sm*ChiA. Both lead to increased accumulation in TG products. In further support of this notion, mutation of Y226 to alanine reduced the TG activity in line with what has been observed for similar mutations in other GH18 chitinases[12, 25].

While the present results show that the TG activity of different GH18 chitinases may be enhanced by similar types of mutations, and thus reveal general principles of TG activity, our study also reveals conspicuous differences between *Sp*ChiD and *Sm*ChiA. *Sm*ChiA is a well-known powerful chitin-degrading enzyme with an essential role in the chitinolytic machinery of *S. marcescens*[47, 48]. Even the D313N mutant of this enzyme still has so much hydrolytic power that TG products are converted to chitobiose and chitotriose[12]. The high level of chitotriose detected for some of the *Sm*ChiA mutants described here indicated considerable TG activity, which could be exploited in the synthesis of glyco-conjugates that are not susceptible to subsequent hydrolysis. Recent functional studies of an *Sp*ChiD homologue from *S. marcescens* showed that this enzyme has little chitin-degrading ability and that it not dominant in the enzyme cocktail that *S. marcescens* secretes when growing on chitin[47]. Tuveng *et al*., 2017,[47] concluded that the biological function of

*Sp*ChiD remains unknown, and one may speculate whether the high TG activity of the wild-type enzyme (described for *Sp*ChiD[13]) is part of its biological function. Clearly, *Sp*ChiD provided a very nice scaffold for engineering efficient transglycosylating enzymes as we were able to generate mutants that produce high and stable levels of longer TG products (Fig. 5).

The conspicuous differences between *Sp*ChiD and *Sm*ChiA may also be a result of the difference in polymer-end specificity. *Sm*ChiA degrades the carbohydrate polymer from the reducing end and *Sm*ChiB from the non-reducing end.[49, 50] Even though these *S. marcescens* chitinases employ the same catalytic machineries and have identical or highly similar residues in the active sites, the end-specificity results in clear differences in thermodynamics of substrate binding and rate of substrate degradation.[41, 51] This is because carbohydrate interactions in positive subsites in *Sm*ChiA facilitates product displacement while they are critical for keeping the substrate bound during hydrolysis in *Sm*ChiB and *vice versa* for negative subsites.[52] The end-specificity has not been determined for *Sp*ChiD. Still, a comparison of the crystal structure of *Sp*ChiD to those of *Sm*ChiA and *Sm*ChiB, suggest that the directionality of *Sp*ChiD resembles *Sm*ChiB more than *Sm*ChiA. This because both *Sm*ChiB and *Sp*ChiD have aromatic residues in subsites +3 (Phe-190 and Trp-290, respectively) where *Sm*ChiA interactions with the +3 sugar moiety is proposed to take place through hydrogen bonds directly or through via water molecules. Moreover, for *Sp*ChiD this path of exposed aromatic residues continues to subsite +4/5 while it goes all the way the way down onto the carbohydrate-binding module for *Sm*ChiB. For *Sm*ChiA, a similar path is observed on negative subsites.[20, 34, 37, 42] To this regards, it is interesting to observe that mutation of Asp^{140} in the conserved DXDXE motif to alanine resulted in an increased TG activity for *Sm*ChiB, but not in *Sm*ChiA.[12]

Conclusion

The TG efficiency of wild-type chitinases (and other GHs) is inevitably limited by enzyme-catalyzed (secondary) hydrolysis of the product. So, to generate longer chain oligosaccharides, there is a need for curtailing the hydrolytic activity while improving TG activity. Previously, several studies have shown that lowering the rate of hydrolysis and increasing the hydrophobicity/sugar acceptor binding surface area result in an increase in TG products. The present results clearly show that site-directed mutagenesis of residues that are involved in fine-tuning catalysis and that may affect the stability, conformation and orientation of intermediates,

can lead to increased TG activity. The combination of such mutations with mutations affecting subsite affinities yielded even higher degree of TG product formations and led to the generation of GH18 variants with high and unprecedented TG activity.

Conflict of interest:

The authors declare that they have no conflicts of interest with the contents of this article.

Acknowledgements

This work was supported by grants 221576, 247001 and 247730 from the Norwegian Research Council – Norway (VGHE, MS and BD) and the South-Eastern Norway Regional Health Authorities, through Grant 2015095 to the Regional Core Facility for Structural Biology (BD), and the DST-INSPIRE-Faculty award (IFA16-LSPA 40) (JM). We also thank the European Synchrotron Radiation Facility for beamtime (project MX-1789) and staff at beamline ID30A-1 for assistance.

Abbreviations:

GHs: Glycosyl hydrolases; CHOS: Chitooligosaccharides; TG: Transglycosylation; GlcNAc: *N*-acetylglucosamine; *Sp*ChiD: Chitinase D from *Serratia proteamaculans*; *Sm*ChiA: Chitinase A from *S. marcescens*.

References:

1. Tharanathan, R. N., and Kittur, F. S. (2003) Chitin — The undisputed biomolecule of great potential, *Crit. Rev. Food Sci. Nutr. 43*, 61-87.
2. Aam, B. B., Heggset, E. B., Norberg, A. L., Sørlie, M., Vårum, K. M., and Eijsink, V. G. H. (2010) Production of chitooligosaccharides and their potential applications in medicine, *Mar. Drugs 8*, 1482.
3. Jeon, Y.-J., Park, P.-J., and Kim, S.-K. (2001) Antimicrobial effect of chitooligosaccharides produced by bioreactor, *Carbohydr. Polym. 44*, 71-76.
4. Prashanth, K. H., and Tharanathan, R. (2005) Depolymerized products of chitosan as potent inhibitors of tumor-induced angiogenesis, *Biochim. Biophys. Acta 1722*, 22-29.
5. Xu, J., Zhao, X., Han, X., and Du, Y. (2007) Antifungal activity of oligochitosan against *Phytophthora capsici* and other plant pathogenic fungi *in vitro*, *Pest. Biochem. Physiol. 87*, 220-228.

6. Rahman, M. H., Shovan, L. R., Hjeljord, L. G., Aam, B. B., Eijsink, V. G., Sørlie, M., and Tronsmo, A. (2014) Inhibition of fungal plant pathogens by synergistic action of chito-oligosaccharides and commercially available fungicides, *PLoS One 9*, e93192.
7. Rahman, M. H., Hjeljord, L. G., Aam, B. B., Sørlie, M., and Tronsmo, A. (2015) Antifungal effect of chito-oligosaccharides with different degrees of polymerization, *Eur. J. Plant Pathol. 141*, 147-158.
8. Ngo, D.-N., Kim, M.-M., and Kim, S.-K. (2008) Chitin oligosaccharides inhibit oxidative stress in live cells, *Carbohydr. Polym. 74*, 228-234.
9. Hamel, L.-P., and Beaudoin, N. (2010) Chitooligosaccharide sensing and downstream signaling: contrasted outcomes in pathogenic and beneficial plant–microbe interactions, *Planta 232*, 787-806.
10. Aguilera, B., Ghauharali-van der Vlugt, K., Helmond, M. T., Out, J. M., Donker-Koopman, W. E., Groener, J. E., Boot, R. G., Renkema, G. H., van der Marel, G. A., and van Boom, J. H. (2003) Transglycosidase activity of chitotriosidase improved enzymatic assay for the human macrophage chitinase, *J. Biol. Chem. 278*, 40911-40916.
11. Umekawa, M., Huang, W., Li, B., Fujita, K., Ashida, H., Wang, L.-X., and Yamamoto, K. (2008) Mutants of *Mucor hiemalis* endo-β-N-acetylglucosaminidase show enhanced transglycosylation and glycosynthase-like activities, *J. Biol. Chem. 283*, 4469-4479.
12. Zakariassen, H., Hansen, M. C., Jøranli, M., Eijsink, V. G., and Sørlie, M. (2011) Mutational effects on transglycosylating activity of family 18 chitinases and construction of a hypertransglycosylating mutant, *Biochemistry 50*, 5693-5703.
13. Madhuprakash, J., Tanneeru, K., Purushotham, P., Guruprasad, L., and Podile, A. R. (2012) Transglycosylation by chitinase D from *Serratia proteamaculans* improved through altered substrate interactions, *J. Biol. Chem. 287*, 44619-44627.
14. Madhuprakash, J., Bobbili, K. B., Moerschbacher, B. M., Singh, T. P., Swamy, M. J., and Podile, A. R. (2015) Inverse relationship between chitobiase and transglycosylation activities of chitinase-D from *Serratia proteamaculans* revealed by mutational and biophysical analyses, *Sci. Rep. 5: 15657*.
15. Das, S. N., Madhuprakash, J., Sarma, P., Purushotham, P., Suma, K., Manjeet, K., Rambabu, S., Gueddari, N. E. E., Moerschbacher, B. M., and Podile, A. R. (2015) Biotechnological approaches for field applications of chitooligosaccharides (COS) to induce innate immunity in plants, *Crit. Rev. Biotechnol. 35*, 29-43.
16. Ly, H. D., and Withers, S. G. (1999) Mutagenesis of glycosidases, *Annu. Rev. Biochem. 68*, 487-522.
17. Williams, S. J., and Withers, S. G. (2000) Glycosyl fluorides in enzymatic reactions, *Carbohydr. Res. 327*, 27-46.
18. Terwisscha van Scheltinga, A. C., Armand, S., Kalk, K. H., Isogai, A., Henrissat, B., and Dijkstra, B. W. (1995) Stereochemistry of chitin hydrolysis by a plant chitinase/lysozyme and x-ray structure of a complex with allosamidin evidence for substrate assisted catalysis, *Biochemistry 34*, 15619-15623.
19. Tews, I., Terwisscha van Scheltinga, A. C., Perrakis, A., Wilson, K. S., and Dijkstra, B. W. (1997) Substrate-assisted catalysis unifies two families of chitinolytic enzymes, *J. Am. Chem. Soc. 119*, 7954-7959.

20. van Aalten, D. M., Komander, D., Synstad, B., Gåseidnes, S., Peter, M. G., and Eijsink, V. G. (2001) Structural insights into the catalytic mechanism of a family 18 exo-chitinase, *Proc. Natl. Acad. Sci. U.S.A. 98*, 8979-8984.
21. Synstad, B., Gåseidnes, S., Van Aalten, D. M., Vriend, G., Nielsen, J. E., and Eijsink, V. G. (2004) Mutational and computational analysis of the role of conserved residues in the active site of a family 18 chitinase, *FEBS J. 271*, 253-262.
22. Aronson, N. N., Halloran, B. A., Alexeyev, M. F., Zhou, X. E., Wang, Y., Meehan, E. J., and Chen, L. (2006) Mutation of a conserved tryptophan in the chitin-binding cleft of *Serratia marcescens* chitinase A enhances transglycosylation, *Biosci. Biotechnol. Biochem. 70*, 243-251.
23. Martinez, E. A., Boer, H., Koivula, A., Samain, E., Driguez, H., Armand, S., and Cottaz, S. (2012) Engineering chitinases for the synthesis of chitin oligosaccharides: Catalytic amino acid mutations convert the GH-18 family glycoside hydrolases into transglycosylases, *J. Mol. Catal. B Enzym. 74*, 89-96.
24. Sirimontree, P., Suginta, W., Sritho, N., Kanda, Y., Shinya, S., Ohnuma, T., and Fukamizo, T. (2014) Mutation strategies for obtaining chitooligosaccharides with longer chains by transglycosylation reaction of family GH18 chitinase, *Biosci. Biotechnol. Biochem. 78*, 2014-2021.
25. Taira, T., Fujiwara, M., Dennhart, N., Hayashi, H., Onaga, S., Ohnuma, T., Letzel, T., Sakuda, S., and Fukamizo, T. (2010) Transglycosylation reaction catalyzed by a class V chitinase from cycad, *Cycas revoluta*: a study involving site-directed mutagenesis, HPLC, and real-time ESI-MS, *Biochim. Biophys. Acta 1804*, 668-675.
26. Umemoto, N., Ohnuma, T., Mizuhara, M., Sato, H., Skriver, K., and Fukamizo, T. (2012) Introduction of a tryptophan side chain into subsite+ 1 enhances transglycosylation activity of a GH-18 chitinase from *Arabidopsis thaliana*, AtChiC, *Glycobiology 23*, 81-90.
27. Umemoto, N., Ohnuma, T., Osawa, T., Numata, T., and Fukamizo, T. (2015) Modulation of the transglycosylation activity of plant family GH18 chitinase by removing or introducing a tryptophan side chain, *FEBS Lett. 589*, 2327-2333.
28. Madhuprakash, J., Tanneeru, K., Karlapudi, B., Guruprasad, L., and Podile, A. R. (2014) Mutagenesis and molecular dynamics simulations revealed the chitooligosaccharide entry and exit points for chitinase D from *Serratia proteamaculans*, *Biochim. Biophys. Acta 1840*, 2685-2694.
29. Madhuprakash, J., El Gueddari, N. E., Moerschbacher, B. M., and Podile, A. R. (2015) Catalytic efficiency of chitinase-D on insoluble chitinous substrates was improved by fusing auxiliary domains, *PLoS One 10*, e0116823.
30. Kabsch, W. (2010) XDS, *Acta Crystallogr. D Biol. Crystallogr. 66*, 125-132.
31. Evans, P. R., and Murshudov, G. N. (2013) How good are my data and what is the resolution?, *Acta Crystallogr. D Biol. Crystallogr. 69*, 1204-1214.
32. Winn, M. D., Ballard, C. C., Cowtan, K. D., Dodson, E. J., Emsley, P., Evans, P. R., Keegan, R. M., Krissinel, E. B., Leslie, A. G., and McCoy, A. (2011) Overview of the CCP4 suite and current developments, *Acta Crystallogr. D Biol. Crystallogr. 67*, 235-242.
33. Adams, P. D., Afonine, P. V., Bunkóczi, G., Chen, V. B., Davis, I. W., Echols, N., Headd, J. J., Hung, L.-W., Kapral, G. J., and Grosse-Kunstleve, R. W. (2010) PHENIX: a comprehensive Python-based system for macromolecular structure solution, *Acta Crystallogr. D Biol. Crystallogr. 66*, 213-221.

34. Madhuprakash, J., Singh, A., Kumar, S., Sinha, M., Kaur, P., Sharma, S., Podile, A. R., and Singh, T. P. (2013) Structure of chitinase D from *Serratia proteamaculans* reveals the structural basis of its dual action of hydrolysis and transglycosylation, *Int. J. Biochem. Mol. Biol. 4*, 166-178.
35. Emsley, P., Lohkamp, B., Scott, W. G., and Cowtan, K. (2010) Features and development of Coot, *Acta Crystallogr. D Biol. Crystallogr. 66*, 486-501.
36. Loose, J. S., Forsberg, Z., Fraaije, M. W., Eijsink, V. G., and Vaaje-Kolstad, G. (2014) A rapid quantitative activity assay shows that the *Vibrio cholerae* colonization factor GbpA is an active lytic polysaccharide monooxygenase, *FEBS Lett. 588*, 3435-3440.
37. Perrakis, A., Tews, I., Dauter, Z., Oppenheim, A. B., Chet, I., Wilson, K. S., and Vorgias, C. E. (1994) Crystal structure of a bacterial chitinase at 2.3 Å resolution, *Structure 2*, 1169-1180.
38. Chen, L., Liu, T., Zhou, Y., Chen, Q., Shen, X., and Yang, Q. (2014) Structural characteristics of an insect group I chitinase, an enzyme indispensable to moulting, *Acta Crystallogr. D Biol. Crystallogr. 70*, 932-942.
39. Kuusk, S., Sørlie, M., and Väljamäe, P. (2015) The predominant molecular state of bound enzyme determines the strength and type of product inhibition in the hydrolysis of recalcitrant polysaccharides by processive enzymes, *J. Biol. Chem. 290*, 11678-11691.
40. Chen, V. B., Arendall, W. B., Headd, J. J., Keedy, D. A., Immormino, R. M., Kapral, G. J., Murray, L. W., Richardson, J. S., and Richardson, D. C. (2010) MolProbity: all-atom structure validation for macromolecular crystallography, *Acta Crystallogr. D Biol. Crystallogr. 66*, 12-21.
41. Baban, J., Fjeld, S., Sakuda, S., Eijsink, V. G., and Sørlie, M. (2010) The roles of three *Serratia marcescens* chitinases in chitin conversion are reflected in different thermodynamic signatures of allosamidin binding, *J. Phys. Chem. B 114*, 6144-6149.
42. Norberg, A. L., Dybvik, A. I., Zakariassen, H., Mormann, M., Peter-Katalinić, J., Eijsink, V. G., and Sørlie, M. (2011) Substrate positioning in chitinase A, a processive chito-biohydrolase from *Serratia marcescens*, *FEBS Lett. 585*, 2339-2344.
43. Bissaro, B., Monsan, P., Fauré, R., and O'Donohue, M. J. (2015) Glycosynthesis in a waterworld: new insight into the molecular basis of transglycosylation in retaining glycoside hydrolases, *Biochem. J. 467*, 17-35.
44. Kobayashi, S., Kiyosada, T., and Shoda, S.-i. (1996) Synthesis of artificial chitin: irreversible catalytic behavior of a glycosyl hydrolase through a transition state analogue substrate, *J. Am. Chem. Soc. 118*, 13113-13114.
45. Krokeide, I.-M., Synstad, B., Gåseidnes, S., Horn, S. J., Eijsink, V. G., and Sørlie, M. (2007) Natural substrate assay for chitinases using high-performance liquid chromatography: a comparison with existing assays, *Anal. Biochem. 363*, 128-134.
46. Jitonnom, J., Lee, V. S., Nimmanpipug, P., Rowlands, H. A., and Mulholland, A. J. (2011) Quantum mechanics/molecular mechanics modeling of substrate-assisted catalysis in family 18 chitinases: conformational changes and the role of Asp142 in catalysis in ChiB, *Biochemistry 50*, 4697-4711.
47. Tuveng, T. R., Hagen, L. H., Mekasha, S., Frank, J., Arntzen, M. Ø., Vaaje-Kolstad, G., and Eijsink, V. G. (2017) Genomic, proteomic and biochemical analysis of the chitinolytic machinery of *Serratia marcescens* BJL200, *Biochim. Biophys. Acta 1865*, 414-421.

48. Mekasha, S., Byman, I. R., Lynch, C., Toupalová, H., Anděra, L., Næs, T., Vaaje-Kolstad, G., and Eijsink, V. G. (2017) Development of enzyme cocktails for complete saccharification of chitin using mono-component enzymes from *Serratia marcescens*, *Process Biochem. 56*, 132-138.
49. Hult, E.-L., Katouno, F., Uchiyama, T., Watanabe, T., and Sugiyama, J. (2005) Molecular directionality in crystalline β-chitin: hydrolysis by chitinases A and B from *Serratia marcescens* 2170, *Biochem. J. 388*, 851-856.
50. Zakariassen, H., Aam, B. B., Horn, S. J., Vårum, K. M., Sørlie, M., and Eijsink, V. G. (2009) Aromatic residues in the catalytic center of chitinase A from *Serratia marcescens* affect processivity, enzyme activity, and biomass converting efficiency, *J. Biol. Chem. 284*, 10610-10617.
51. Hamre, A. G., Schaupp, D., Eijsink, V. G., and Sørlie, M. (2015) The directionality of processive enzymes acting on recalcitrant polysaccharides is reflected in the kinetic signatures of oligomer degradation, *FEBS Lett. 589*, 1807-1812.
52. Vaaje-Kolstad, G., Horn, S. J., Sørlie, M., and Eijsink, V. G. (2013) The chitinolytic machinery of *Serratia marcescens* - a model system for enzymatic degradation of recalcitrant polysaccharides, *FEBS J. 280*, 3028-3049.